Research Journal of Applied Sciences, Engineering and Technology 12(1): 1-8, 2016
DOI:10.19026/rjaset.12.2297
ISSN: 2040-7459; e-ISSN: 2040-7467

Submitted: November 30, 2014 Accepted: January 23, 2015 Published: January 05, 2016

Research Article

Design and Analysis of a Flywheel Supported by Hybrid Magnetic Bearing

Prince Owusu-Ansah, Hu Yefa and Wu Huachun
Department of Mechanical and Electrical Engineering, Wuhan University of Technology,
P.O. Box No. 205, Luoshi Road, Wuhan, China

Abstract: In this study, a design structure of a new flywheel supported by Hybrid Magnetic Bearing (HMB) with permanent magnet in rotor is modeled using 3D Software solid works. The hybrid magnetic bearing consists of two sets of Active Magnetic Bearing (AMB) and a set of Permanent Magnetic Bearing (PMB) as well as a frequency response analysis for a rotor dynamic system at a rotor speed of 20,000 rpm. In this system an axial PMB is located at the top of the rotor to provide a levitation force in order to suspend more flywheel weight, two radial and axial AMB are added to provide support in the radial and axial directions to improve stiffness by two orders of magnitude from 10^4 N/M to 10^6N/M and the damping of the flywheel energy storage system (FESS). The prototype HMB model flywheel structure presented in Fig. 6 with a storage capacity of 4 KW rotating at a speed of 20000 rpm has an advantage of simplicity in structure, high energy density, low frictional and internal energy losses, ultimately resulting in higher power output. A unique feature of this design is that the upper and the lower ends of the rotor and the stator core have been tapered compared to previous design ensuring that larger thrust and lower radial force are obtained.

Keywords: Active magnetic bearing, flywheel energy storage system, hybrid magnetic bearing, levitation force, permanent magnetic bearing

INTRODUCTION

Flywheel as a mechanical device with significant moment of inertia been used to serve as a kinetic energy storage and retrieval devices existed well over one hundred years ago were attached to an axle solely to store kinetic energy and smoothes the operation of a reciprocating engine during its cycle of operation. Technological advancement has seen the breakthrough of a new kind of hybrid magnetic bearings.

Active Magnetic Bearing (AMB) are clearly favored over passive bearings, because they are actively controlled by means of electromagnet and results in high power loss due to the presence of a biased current, but the inclusion of a suitable feedback control loop and other elements such as sensors and power amplifier makes its more preferably than the passive bearing due to its lack of active control damping capabilities (Filator and Maslen, 2001; Samanta and Hirani, 2008). For these reasons more emphasis is now-biased on hybrid magnetic (HMB), which includes the advantages of both Passive Magnetic Bearing (PMB) and Active Magnetic Bearing (AMB). In Hybrid Magnetic Bearing (HMB) the permanent magnetic generates the bias flux which produces the main supporting force consequently the control current results to low power loss. Different kinds of HMB structure have been discussed in Zmood *et al*. (1997) and Zhu *et al*. (2002), in these structures, the Bias flux and the control flux share the same path, which results to large control current due to the presences of large permanent magnet reluctance, creating high power loss. This work studies the design of hybrid magnetic bearing to support flywheel energy storage systems.

Types of bearings: There are three types of bearings: the active, the passive and the hybrid magnetic bearings. The type of bearing used in a particular system depends on the function that the bearing will be required to perform cost and reliability.

Passive bearing: A passive magnetic bearing consists of a permanent magnetic placed in a position that can levitate an object in this case the rotor making it contact free.

There are two ways to obtain the electromagnetic force. The magnets can be placed in order to attract the object or by putting two or more magnetic repelling the piece. In addition, the magnets can be displayed in two different ways: radial and vertical. Radial bearings are being studied for application, but became very difficult

Corresponding Author: Prince Owusu-Ansah, Department of Mechanical and Electrical Engineering, Wuhan University of Technology, P.O. Box No. 205, Luoshi Road, Wuhan, China

to design them due to the earth gravity (Sung *et al*., 2001).

There are few advantages using PMB. These advantages are economical, practical and of reliability. PMB is considered an economic solution because it has no inherent cost for it operation due to the fact that there are no active circuits. So, the energy consumption is insignificant. This type of bearing is practical because when compared to other types, it does experience energy losses, does not need position sensors and coils. Its construction and design is therefore simple and does not require maintenance as well as any type of hardware installation or control mechanism. However the disadvantages related to PMB is that if instability occurs, there is no way to bring the system into balance state. For systems requiring high performance, active magnetic bearings are the best choice.

Active Magnetic Bearing (AMB): The AMB is composed of a copper coil or in some cases high temperature superconductors which will provide the magnetic flux ensuring the contact free between the pieces in these design, the latter is adopted and model using 3D solid work was used to design the radial and axial magnetic bearings. AMB has good performance and with a microprocessor control based it compensates any instability that occurs in the system, due to the AMB biased current the energy losses of this type of bearing are very high as a result of this fact some AMB have been replaced by PMB and AMB are starting to use HSTC, which are more efficient.

Hybrid Magnetic Bearing (HMB): A design structure of a 4KW storage capacity rotating at a speed of 20000 rpm HMB is to be module with permanent magnet in rotor (Yueqin and Yanliang, 2004) using three dimensional (3-D) modelling software solid works.

The hybrid magnetic bearing consists of a set of two AMB and a set of PMB. In this system an axial PMB is located at the top of the rotor to provide a levitation force in order to suspend more flywheel weight (Schweitzer *et al*., 1994) two radial and axial AMB are added in the radial and axial directions. The upper and the lower ends of the rotor and the stator core have been tapered as compared to most designs, the overlap areas between the stator and the rotor core is increased, this ensures that larger thrust and lower radial forces are obtained. Permanent magnet guarantees the support for contact free system of the spinning wheel. A sensor gap coupled with a power system compensates the instabilities that can be observed, so in this type of bearing, the performance of an AMB and control is guaranteed without the kind of losses of a pure AMB.

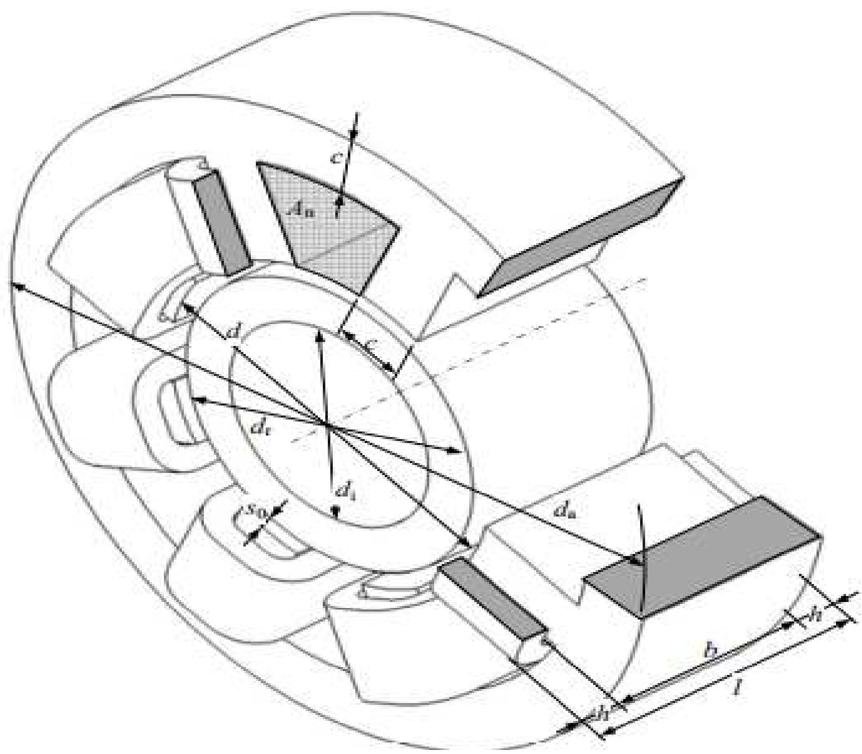

Fig. 1: Typical geometry of the radial magnetic bearing; d: Inner diameter (bearing diameter); d_a: Outer diameter, di: Shaft diameter; c: Leg width; h: Winding head height; b: bearing width (magnetically active); d_r: Rotor diameter; A_n: Slot cross section (winding space); S_o: Nominal air gap

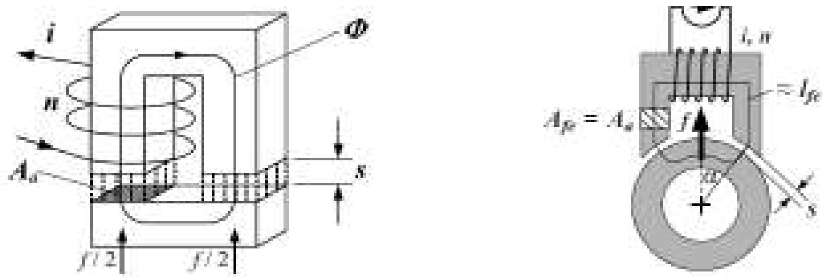

(a) Force (b) Geometry

Fig. 2: Force and geometry of a radial magnet

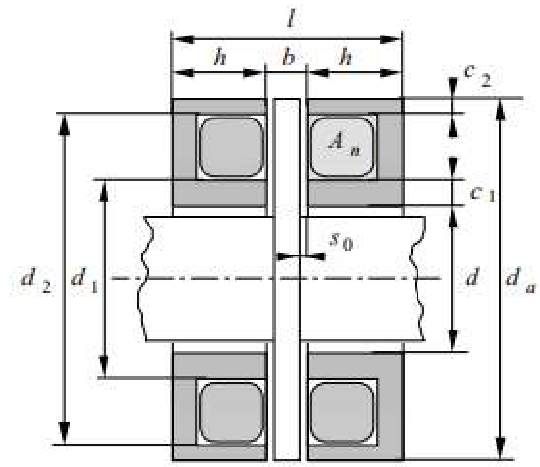

Fig. 3: Geometry of a typical axial magnetic bearing; d: Inner diameter (or bearing diameter); da: Outer diameter c1: Inner leg width d_1: Inner winding space diameter; d_2: Outer winding space diameter; A_n: Slot cross section (winding space); S_o: Nominal air gap; c_2: Outer leg width; *l*: bearing length; h_n: Slot depth

MATERIALS AND METHODS

Radial magnetic bearing design: Figure 1 shows the geometric parameters of a typical radial bearing magnet. At least three coils are necessary for a complete radial magnet bearing in order to generate forces in two perpendicular directions. However the most common design uses four independent coils, for each direction two opposite pairs of electric coils are used.

When optimizing the bearing geometry the leg width C in Fig. 2 of the magnet pole can be varied with a larger leg width, the slot cross section A_n, is reduced, as well as the admissible magneto motive force NI_{max}. Both an increase in leg width (increases of the iron cross-section) and reduction of NI reduces the flux density path with the leg width.

In contrast to forces acting on conductors in a magnetic field (Lorentz force), the attraction force of magnets is generated at the boundaries between differing permeability μ. Considering the energy W_a in the volume of air gap, $V_a = 2SA_n$. In the case of the homogeneous field in the air gap of the magnetic loop, the stored energy W_a obeys:

$$W_a = \frac{1}{2} B_a H_a V_a = \frac{1}{2} B_a H_a A_n (2S) \qquad (1)$$

The force acting on the ferromagnetic body ($\mu_r \gg 1$) is generated by a change of the field energy in the air gap, as a function of the body displacement. For small displacement ds the magnetic flux $B_a A_n$ remains constant.

When the air gap S increases byds, the volume $V_a = 2SA_n$ increases and the energy W_a in the field increases by dW_a.

Table 1 shows the parameters of the radial magnetic bearing (AMB).

Axial magnetic bearing design: Figure 3 illustrates the geometry of a typical axial magnetic bearing. An important design consideration for the axial bearing magnet is to balance the radial thickness of the inner and outer legs so that they both saturate at approximately the same coil current.

First the pole area is defined for the inner pole:

$$A_p = \frac{\pi(d_1^2 - d^2)}{4} \qquad (2)$$

Table 1: Parameters of the radial magnetic bearing AMB

F_{design}	350 N
Bias current	1.5
Number of turns per coil	220
Nominal air gap so	0.5
Relative permeability of free space, μo	$4\pi \times 10^{-7}$
B_{max}	$1.2T < B_{sat}$
Maximum magnetic induction (T)	1.2
Maximum current in each coil	6A
Magnetic flow cross sectional A	450 mm^2
Nominal magnetic inductivity	20 Mh
Outer diameter	100 mm
Inner diameter	40 mm
Bearing length	45 mm
Operational speed	20,000 rpm

Table 2: Parameters of the Axial Magnetic Bearing (AMB)

F_{design}	350 N
Bias current	2.0 A
Number of turns per coil	220
Nominal air gap so	0.5
Relative permeability of free space, μo	$4\pi\times10^{-7}$
B_{max}	$1.2T < B_{sat}$
Maximum magnetic induction (T)	1.2
Maximum current in each coil	6 A
Magnetic flow cross section A	350 mm^2
Nominal magnetic inductivity	16 Mh
Outer diameter	60 mm
Inner diameter	20 mm
Bearing length	80 mm
Operational speed	20000 rpm

Fig. 4: Photograph of AMB rotor model

Neglecting flux leakage and other non-idealities, the balanced pole area condition is achieved when:

$$A_p = \frac{\pi(d_a^2 - d_2^2)}{4} \tag{3}$$

The radial component of the stator needs to have a minimum area matching that of the pole faces:

$$A_p = \frac{\pi d_1(l - b - 2h_n)}{2} \tag{4}$$

For an axial direction only one pair of opposite coil is necessary since there is no magnetic reversal during rotation of the rotor's thrust disk, each of the two axial magnetic bearing units (upper and lower units for the vertically suspended rotor) are design as a pot-shaped magnet. The parameters for the bearing is shown below in Table 2.

Figure 4 shows the design photograph of the Active Magnetic Bearing (AMB) rotor using solid works model.

Flywheel rotor design: The rotational inertia of the flywheel is:

$$J = \frac{1}{2}m(r_o^2 + r_i^2) \text{ Mass is } m = \pi\rho h(r_o^2 - r_i^2) \tag{5}$$

where, h means the thickness of flywheel panel, r_0, r_i means the internal and external radius of flywheel panel, ω is the revolving speed of flywheel panel. So, the energy which this flywheel can host should be as follow:

$$\begin{aligned} E &= \frac{1}{2}J\omega^2 = \frac{1}{4}m(r_o^2 + r_i^2)\omega^2 \\ &= \frac{1}{4}\pi\rho h(r_o^2 - r_i^2)(r_o^2 + r_i^2)\omega^2 \\ &= \frac{1}{4}\pi\rho h\omega^2 r_o^2(1 - (\frac{r_i}{r_o})^4) \\ &= \frac{1}{4}\pi\rho h\omega^2 r_o^2(1 - k^4) \end{aligned} \tag{6}$$

where, $k = \frac{r_i}{r_o}$. It is obvious that E is not only relating to ω and material, but also relating to h, r_0 and r_i. Energy storage density of the flywheel is:

$$u = \frac{E}{m} = \frac{1}{4}(r_o^2 + r_i^2)\omega^2 = \frac{1}{4}r_o^2\omega^2(1 + k^2) \tag{7}$$

Rotor materials: The materials that compose the flywheel rotor will limit its rotational speed; due to the tensile strength develop. Lighter materials develop lower inertial loads at a given speed, therefore composites materials, with low density and high tensile strength, are good material choice for high speed, high energy density flywheel, but it must be clearly stated that designing a flywheel in composites requires a good understanding of the basic concept of composite materials which could be discussed into more detailed in subsequent future work.

Carbon composite materials are a new generation of materials that are lighter, stronger and which can maximize higher energy density than the convectional ones such as the steel. A cross-sectional view of a high speed rotor to be model and analysis consisting of (1) Shaft, (2) Outer shell, (3) Inner shell and (4) Flange as shown in Fig. 5.

Rotor vibrations: A rotor may tend to vibrate in any directions, these vibrations falls under anyone of the following types:

- Lateral
- Torsional
- Axial

Lateral vibration occurs in radial plane of the rotor spin axis it causes dynamic bending of the shaft in two mutually perpendicular lateral plane. The natural frequencies of lateral vibration are influenced by rotating speed of the rotor hence the overwhelming number of rotordynamic analysis and design are mostly focused only on lateral vibration.

In rotating system such as high speed rotors, the ratio of bearing stiffness to the shaft stiffness has a greater influence on modes shapes. The bearing stiffness k, for the sake of simplicity, is equal at all bearing positions and thus the following relations for the bearing force holds:

$$\mathrm{f} = -\mathrm{k}\begin{bmatrix} x_a \\ y_a \\ x_b \\ y_b \end{bmatrix} = -\mathrm{k}\begin{bmatrix} a & 1 & 0 & 0 \\ b & 1 & 0 & 0 \\ 0 & 0 & a & 1 \\ 0 & 0 & b & 1 \end{bmatrix} z \tag{8}$$

$$\mathrm{Z} = \mathrm{Bf} = -\mathrm{k}\begin{bmatrix} a^2+b^2 & a+b & 0 & 0 \\ a+b & 2 & 0 & 0 \\ 0 & 0 & a^2+b^2 & a+b \\ 0 & 0 & a+b & 2 \end{bmatrix} z = -Kz \tag{9}$$

This finally leads to the general form of equation of motion for all vibration problems as:

$$[M]\{\ddot{z}\} + [C]\{\dot{z}\} + [K]\{z\} = \{f\} \tag{10}$$

where,
$[M]$ = Symmetric mass matrix
$[C]$ = Symmetric damping matrix
$[K]$ = Symmetric stiffness matrix
$\{f\}$ = External force vector
$\{Z\}$ = Generalized coordinate vector

In rotor dynamics, this equation of motion can be expressed in the general form as (Genta, 2005):

$$[M]\{\ddot{z}\} + ([C] + [Cgyro])\{\dot{z}\} + ([K] + [H])\{z\} = \{f\} \tag{11}$$

Equation (10) describes the motion of an axially symmetric rotor, which is rotating at constant spin speed Ω about it spin axis.

The gyroscopic and circulatory matrices $[Cgyro]$ and [H] are greatly influenced by rotational velocity Ω, tends to zero, the skew-symmetric terms presents in Eq. (10) vanish and represent an ordinary stand still structure.

In general, the translatory motions x_s, y_s and the angular motions α, β will be coupled. In addition to that, the motions in the $x_I z_I - plane$ will be coupled with the motion in the $y_I z_I -$ plane, if the rotor speed $\Omega \neq 0$.

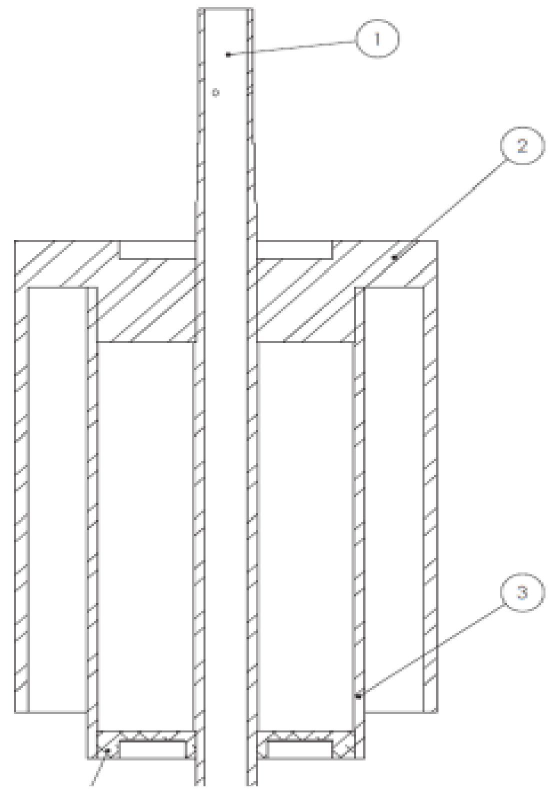

Fig. 5: Cross section of rotor


Fig. 6: Photograph of flywheel model

RESULTS AND ANALYSIS

Rotor dynamic analysis: The frequency response for the rotor dynamic system was measured at different rotor speed up to a maximum of 20,000 rpm in order to under study the dynamic system behavior.

When the shaft was modelled by finite elements, the natural frequencies and the mode shapes of the rotor system at speed Ω = 0 was calculated, after this influences of the rotational speed at various stages was investigated up to a maximum of 20,000 rpm which showed that increasing rotor rotational speed influences the behavior of the natural frequencies and mode shapes due to the gyroscopic moments of elements with high moments of inertia.

Figure 6 shows a Campbell diagram of natural frequency against natural frequency. The points where

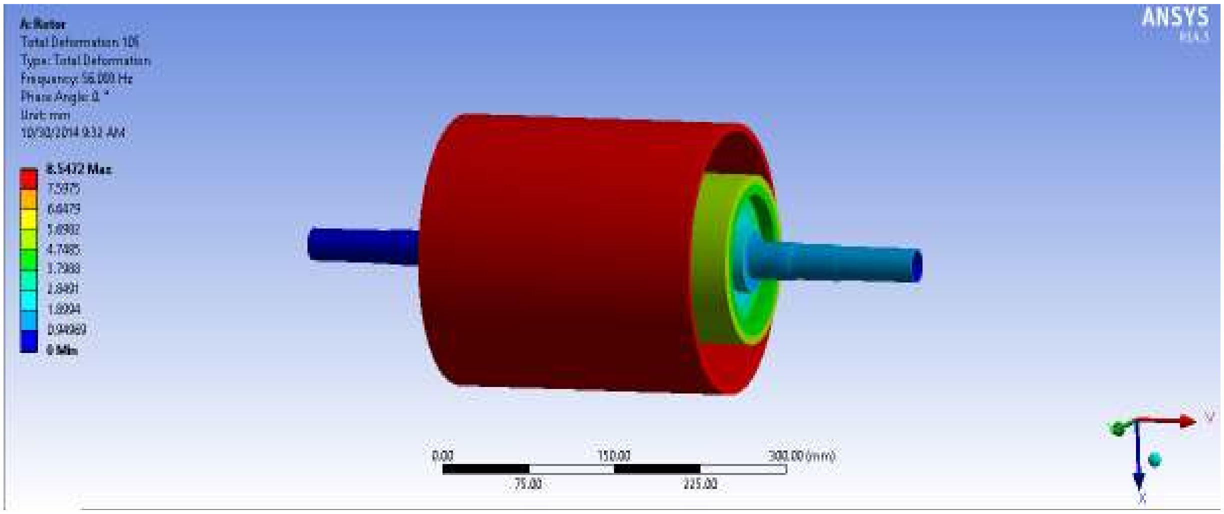

Fig. 7a: Total deformation of rotor model

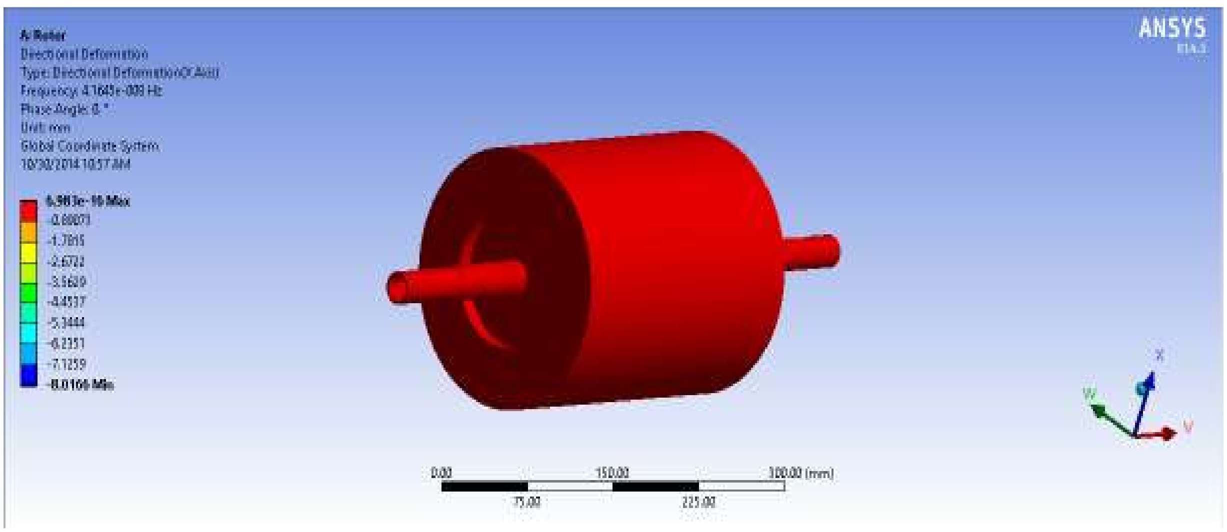

Fig. 7b: Directional deformation of rotor model

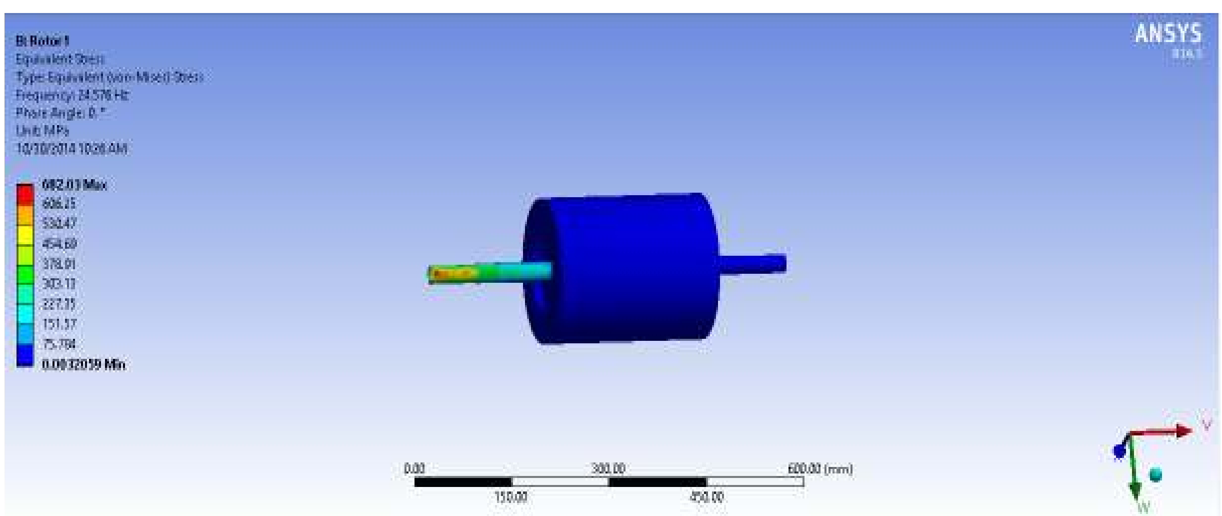

Fig. 7c: Equivalent stress of rotor model

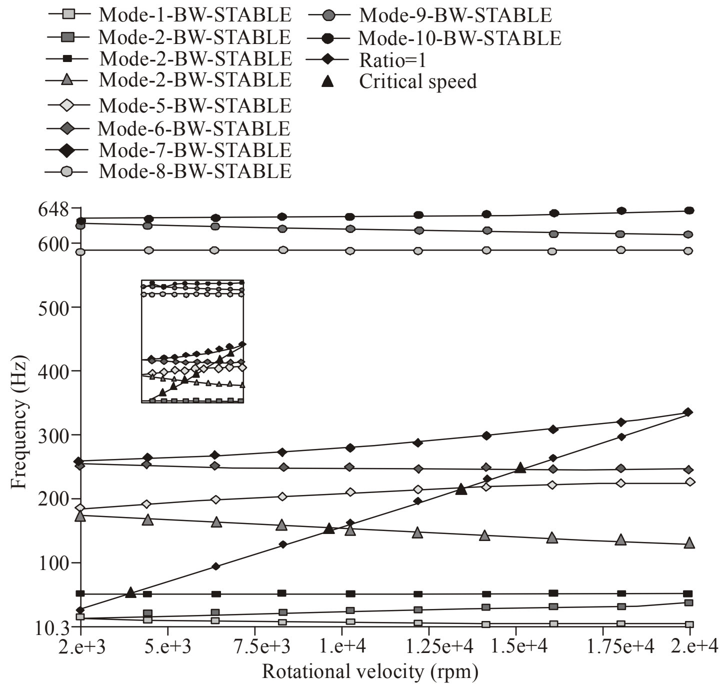

Fig. 8: Campbell diagram of rotor

this lines crosses the natural frequency curves shows where the resonances are expected. Of particular importance are the intersections with the forward frequency curves, due to the fact that the unbalance excitation forces are able to excite these forward natural frequencies.

It can be seen that because of the gyroscopic effect the natural frequency of whirl (mode) is split into two frequencies (modes) when the rotor speed is not zero. As the rotor speed increases the gyroscopic moment stiffens the rotor stiffness of the forward whirl and weakens the rotor stiffness of the backward whirl resulting in the gyroscopic moment to shift up the forward whirl frequencies and shifts down the backward whirl frequencies.

A main identification technique was to excite the system under consideration with known forces (input) and to measure the response (output) and to use the measured input and output relations to identify unknown system properties. One of the main obstacles to this study was with the identification techniques in the rotor dynamics in the excitation of a rotating structure during the rotor operation.

Investigation revealed that Active Magnetic Bearing (AMB) can be used to solve this difficult task. These new techniques appear to be more promising because AMB's do not only support the rotor, but acts as excitation and force measurement equipment.

The models in Fig. 7a to c shows a Three dimensional FEM analysis models for a rotor used in a new HMB.

Critical speed and Campbell diagram analysis: In this analysis, a number of damped frequency analyses are performed on the rotor model for the speed range starting from 0 rpm to 20000 rpm with an increment of 500 rpm using multiple load steps. Since the model undergoes rotation in this analysis, it is possible to extract damped frequency at any speed between the specified speed ranges with the defined increment.

The frequency variation corresponding to the different rotational speeds are determined from this analysis and these variations are plotted in the Campbell diagram shown in Fig. 8 obtained from ansys results. It is observed from the Campbell diagram that forward whirl frequencies increases and the backward whirl frequencies decreases with increase in rotational speed, an extra line can line corresponding to the rotational frequency cross over the modal frequency line. The critical speeds of the rotor are calculated at various interference points of the modal frequency lines and excitation line as shown in the Campbell diagram Fig. 8.

We could find that there are four critical speeds corresponding to the modes about and below 500 rpm and from this the FESS was expected to run up to 20000 rpm without any severe vibration problems which satisfies our design goal to store usable energy of 4 KW.

CONCLUSION

A flywheel structure supported by Hybrid Magnetic Bearing (HMB) which consists of AMB and PMB was designed and built using solid works software for the Flywheel Energy Storage System (FESS). The design and specification of the system were described.

The magnetic bearing was designed to fit into the inner radius of the wheel developed in Fig. 5. A unique feature of this design is that the upper and lower ends of the rotor and stator core have been tapered compared to most design ensuring that larger thrust and lower radial forces are obtained. The magnetic bearing has two distinct circuits; the passive and the active bearing. The active bearing was designed with the purpose of helping the passive bearing, when the passive bearing cannot sustain the wheel or maintain the wheel on its right position.

The magnetic bearing has a cylindrical shape which fits into the inner radius of the wheel, it’s also consists of a permanent magnet and a coil of which one is the passive bearing and the other is the active bearing. The bearing is composed of by two pieces: the fixed one (the upper part that has the permanent magnet and the active bearing and the downward pieces fixed to the wheel, which function is to close the flux path, being made of ferromagnetic materials.

Hybrid Magnetic Bearing (HMB) combines the benefits of a passive magnetic bearing (no energy losses) and the benefits of an active bearing (control and stability). Hybrid magnetic bearing incorporates permanent magnet which compensate for gravitation and levitation force (Teshima *et al*., 1997) there by providing a promising way of resolving the difficulties associated with Flywheel Energy Storage Systems (FESS).

Frequency response analysis for the rotor dynamic system as well as critical speed and Campbell diagram analysis which were performed at different rotor speed up to a maximum speed of 20,000 rpm without any severe vibration problems encountered which satisfies our goal design to store usable energy of 4 KW. It could also be observed Successive increase in rotational rotor speed influences the behavior of the natural frequencies and mode shapes due to gyroscopic moments of elements with high moment of inertia.

REFERENCES

Filator, A.V. and E.H. Maslen, 2001. Passive magnetic bearing for flywheel energy storage system. IEEE T. Magn., 37(6): 3913-3924.

Genta, G., 2005. Dynamics of Rotating Systems. Springer, New York.

Samanta, P. and H. Hirani, 2008. Magnetic bearing configurations: Theoretical and experimental studies. IEEE T. Magn., 44(2): 292-300.

Schweitzer, G., H. Bleuler and A. Traxler, 1994. Active Magnetic Bearings: Basics, Properties and Applications of Active Magnetic Bearings. Verlag der Fachvereine, Zurich, Switzerland, pp: 48-60.

Sung, T.H., J.S. Lee, Y.H. Han, S.C. Han, C.J. Kim, G.W. Hong *et al*., 2001. Flywheel energy storage system with a horizontal axle mounted on high Tc superconductor bearings. Cryogenics, 41(7): 461-467.

Teshima, H., T. Tawara, J. Kobuchi, T. Suzuki and R. Shimada, 1997. Ring-shaped flywheel energy storage systems with superconducting levitation. Proceeding of the Power Conversion Conference. Nagaoka, 2: 701-706.

Yueqin, D. and X. Yanliang, 2004. A new hybrid-type permanent magnet biased magnetic bearing with rotor magnet. J. Shandong Univ., 34: 46-50.

Zhu, H.Q., S.Q. Yuan, B. Li *et al*., 2002. The working principle and parameter design for permanent magnet biased radial-axial direction magnetic bearing. Proc. CSEE, 22(9): 54-58. (In Chinese)

Zmood, R.B., L.J. Qin, J.A. Kirk and L. Sun, 1997. A magnetic bearing system design methodology and its application to a 50 Wh open core composite flywheel. Proceeding of the 32nd Intersociety Energy Conversion Engineering Conference (IECEC-97), 4: 2306-2311.